Prostaglandins and Other Lipid Mediators 142 (2019) 59–67

Contents lists available at ScienceDirect

Prostaglandins and Other Lipid Mediators

journal homepage: www.elsevier.com/locate/prostaglandins

Low mRNA expression and activity of monoacylglycerol lipase in human SH-SY5Y neuroblastoma cells

Janis Szeremeta[1], Jessica Karlsson, Mireille Alhouayek[2], Christopher J. Fowler*

Department of Pharmacology and Clinical Neuroscience, Umeå University, SE-901 87 Umeå, Sweden

ARTICLE INFO

Keywords:
Monoacylglycerol Llipase
SH-SY5Y cells
Neuroblastoma
Endocannabinoid
DU-145 cells

ABSTRACT

Relatively little is known about the endocannabinoid system in human neuroblastoma cell lines. In the present study, we have investigated the expression of the genes coding for the enzymes involved in the synthesis and catabolism of endocannabinoids in the SH-SY5Y cell line. The expression of *MGLL*, the gene coding for the 2-arachidonoylglycerol hydrolytic enzyme monoacylglycerol lipase (MAGL), was found to be 85 and 340 fold lower than the expression levels for the genes coding for alpha/beta-hydrolase domain containing 6 and 12 (*ABHD6*, *ABHD12*), which are alternative hydrolytic enzymes for this endocannabinoid. In comparison, mRNA levels of *MGLL* were 1.5 fold higher than *ABHD6* and 2 fold lower than the levels of *ABHD12* in DU-145 human prostate cells. In functional assays, the hydrolysis of the 2-arachidonoylglycerol homologue 2-oleoylglycerol by intact SH-SY5Y cells was partially inhibited by the ABHD6 inhibitor WWL70, but not by the MAGL inhibitor JZL184, whereas the reverse was true in DU-145 cells. The combination of JZL184 + WWL70 did, however produce a significantly greater inhibition of 2-OG hydrolysis than seen with WWL70 alone in the SH-SY5Y cells. The low *MGLL* expression in the SH-SY5Y cells was not due to epigenetic silencing, since levels were not affected by treatment with the methylation inhibitor 5-aza-2′-deoxycytidine and/or the histone acetylase inhibitor trichostatin A. The low *MGLL* expression in SH-SY5Y cells should be taken into account when using these cells in experiments investigating the involvement of the endocannabinoid system in models of physiological and pathological processes.

1. Introduction

The endocannabinoid system in its simplest form can be defined as consisting of the endogenous arachidonic acid derivatives 2-arachidonoylglycerol (2-AG) and anandamide (arachidonoylethanolamide, AEA), their target cannabinoid (CB) receptors and their synthetic and catabolic enzymes [1] (schematic, see Fig. 1). The endocannabinoid system is involved in a variety of central and peripheral functions ranging from regulation of pain perception to involvement in reproduction [2]. Endocannabinoids are synthesised “on demand” in response to stimuli such as calcium mobilisation (review, see [3]). As with all signalling molecules, endocannabinoids are effectively catabolised. For AEA, a key hydrolytic enzyme is fatty acid amide hydrolase (FAAH) [4,5], although AEA and other *N*-acylethanolamines are also substrates for *N*-acylethanolamine acid amide hydrolase (NAAA) [3]. 2-AG is also a substrate for FAAH [6], but in the mouse brain, approximately 85% of 2-AG hydrolysis is brought about by monoacylglycerol lipase (MAGL) [7], and MAGL inhibitors produce pronounced increases

Abbreviations: 2-AG, 2-arachidonoylglycerol; 2-OG, 2-oleoylglycerol; AA, arachidonic acid; ABHD6/12, alpha/beta-hydrolase domain containing 6/12; ADAR2, adenosine deaminase acting on RNA of the glutamate receptor 2 subunit B; AEA, anandamide, arachidonoylethanolamide; Aza dC, 5-aza-2′-deoxycytidine (Aza dC); CBR, cannabinoid receptor; COX-2, cyclooxygenase-2; DAG, diacylglycerol; DAGL, diacylglycerol lipase; FAAH, fatty acid amide hydrolase; HPETE-GE / EAs, hydroperoxyeicosatetraenoyl glyceryl ester / ethanolamides; JZL184, 4-nitrophenyl-4-(dibenzo[d] [13]dioxol-5-yl(hydroxy)methyl) piperidine-1-carboxylate; LOX, lipoxygenase; MAGL, monoacylglycerol lipase; NAAA, *N*-acylethanolamine acid amide hydrolase; NAPE, *N*-acyl-phosphatidylethanolamine; NAPE-PLD, NAPE-phospholipase D; PEA, palmitoylethanolamide; PG-EA, prostaglandin ethanolamides (prostamides); PG-GE, prostaglandin glyceryl esters; RPL19, ribosomal protein L19; TSA, trichostatin A; URB597, (3′-(aminocarbonyl)[11′-biphenyl]- 3-yl)-cyclohexylcarbamate; WWL70, *N*-methyl-*N*-[[3-(4-pyridinyl)phenyl] methyl]-carbamic acid 4′-(aminocarbonyl) [11′-biphenyl]-4-yl ester

* Corresponding author.
E-mail address: christopher.fowler@umu.se (C.J. Fowler).
[1] Present address: Eurofins WEJ Contaminants GmbH, Neuländer Kamp 1, Hamburg, DE-21079, Germany.
[2] Present address: Bioanalysis and Pharmacology of Bioactive Lipids Research Group, Louvain Drug Research Institute, Université catholique de Louvain, B1.72.01-1200, Bruxelles, Belgium.

https://doi.org/10.1016/j.prostaglandins.2019.04.003
Received 24 January 2019; Received in revised form 4 April 2019; Accepted 8 April 2019
Available online 09 April 2019
1098-8823/

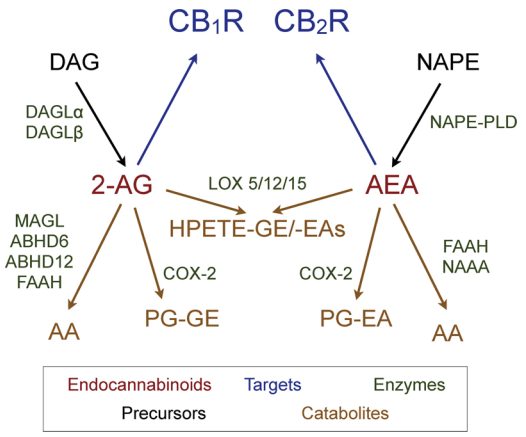

Fig. 1. Schematic of the endocannabinoid target receptors and the synthetic and catabolic enzymes investigated in the present study.
For a detailed description of the canonic and alternative metabolic pathways for the endocannabinoids, see Ueda et al. [3]. Abbreviations: AA, arachidonic acid; ABHD6/12, alpha/beta-hydrolase domain containing 6/12; CBR, cannabinoid receptor; COX-2, cyclooxygenase-2; DAG, diacylglycerol; DAGL, diacylglycerol lipase; FAAH, fatty acid amide hydrolase; HPETE-GE / EAs, hydroperoxyeicosatetraenoyl glyceryl ester / ethanolamides; LOX, lipoxygenase; MAGL, monoacylglycerol lipase; NAAA, *N*-acylethanolamine acid amide hydrolase; NAPE, *N*-acyl-phosphatidylethanolamine; NAPE-PLD, NAPE-phospholipase D; PG-EA, prostaglandin ethanolamides (prostamides); PG-GE, prostaglandin glyceryl esters. The genes coding for the enzymes and CB receptors are given in Table 1.

in brain 2-AG levels with a corresponding decrease in both arachidonic acid and, following lipopolysaccharide treatment, in downstream prostaglandin levels [8,9]. Knockout of either neuronal or astrocytic MAGL results in increased brain 2-AG levels, whereas knockout of microglial MAGL does not affect brain 2-AG levels [10]. MAGL is also found in peripheral tissues, not least adipose tissue, adrenal gland and the kidney [11]. In addition to hydrolysis, the two endocannabinoids can be oxygenated by cyclooxygenase-2 (COX-2) and lipoxygenases, as well, in the case of AEA, by CYP450 enzymes, to produce biologically active compounds [3,12].

From the above discussion, it is reasonable to regard MAGL as a key enzyme in the catabolism of 2-AG and related monoacylglycerols such as 2-oleoylglycerol (2-OG) and MAGL inhibitors have potential use in a variety of disorders including multiple sclerosis, anxiety, inflammatory bowel disease, glaucoma and possibly cancer (e.g. [13–17]). One potential use of such compounds is in the treatment of Parkinson's disease where in mouse models, pharmacological inhibition of MAGL reduces the deleterious effects of the dopaminergic neurotoxin MPTP upon the number of dopaminergic neurons in the nigrostriatal pathway [9,18,19].

In vitro studies of neural cells, their function and their sensitivity to neurotoxicants are greatly aided by the use of neuroblastoma cell lines [20]. The human neuroblastoma cell line SH-SY5Y is a case in point: these cells, which are a subclone of the SK-N-SH cell line derived from a bone marrow metastasis in a 4 year old child, express enzymes associated with catecholaminergic cells [21] and can be differentiated with retinoic acid to a dopaminergic-like neuronal phenotype [22]; as such they are frequently used as a simple in vitro human model for Parkinson's disease [23]. The use of such cells makes the assumption that the system under study resembles that seen in vivo. With respect to the endocannabinoid system, most work in this respect has utilised mouse neuroblastoma cells, but there is evidence that human neuroblastoma cells such as SH-SY5Y cells express the components of the endocannabinoid system and that AEA can produce apoptotic effects [24–29]. To our knowledge, the only available data for the potential role of the endocannabinoid system in protection against the deleterious effects of MPTP in SH-SY5Y cells is the study of Aymerich et al. [29] who reported that MAGL inhibition by 100 nM JZL184 reduced cell death (lactate dehydrogenase release) produced by 24 h exposure to MPP^+, the active metabolite of MPTP, by about 25–50%. This reduction was abolished by a high (1 μM) concentration of the CB_2 receptor antagonist AM630, whereas lower (1.6–200 nM) concentrations of this compound were without effect.

Given the paucity on data in human neuroblastoma cells, we have investigated in the present study the expression of the synthetic and catabolic enzymes involved in 2-AG and AEA turnover in SH-SY5Y neuroblastoma cells. The main finding is that, in contrast to the situation in the central nervous system [7–10], the expression of *MGLL* in these cells is very low relative to other hydrolytic enzyme genes involved in monoacylglycerol hydrolysis, and that its low expression is not due to epigenetic silencing that can occur in transformed cells.

2. Materials and methods

2.1. Drugs and compounds

[^{3}H]2-oleoylglycerol ([^{3}H]2-OG, 60 Ci/mmol, labelled in the glycerol part of the molecule) was obtained from American Radiolabeled Chemicals Inc, St. Louis, MO, USA. JZL184 (4-nitrophenyl-4-(dibenzo[d][1,3]dioxol-5-yl(hydroxy)methyl) piperidine-1-carboxylate), URB597 ((3′-(aminocarbonyl)[1,1′-biphenyl]- 3-yl)-cyclohexylcarbamate) and WWL70 (*N*-methyl-*N*-[[3-(4-pyridinyl)phenyl] methyl]-carbamic acid 4′-(aminocarbonyl) [1,1′-biphenyl]-4-yl ester) were obtained from the Cayman Chemical Co. (Ann Arbor, MI, USA). Pentadecylamine, 5-Aza-2′-deoxycytidine (Aza dC) and Trichostatin A (TSA) were obtained from Sigma-Aldrich (St. Louis, MO, USA).

2.2. Cell culture

Human SH-SY5Y neuroblastoma cells (passage range 19 to 28) were obtained from the European Collection of Authenticated Cell Cultures (Porton Down, UK). Human DU-145 prostate cancer cells (passage range 17 to 29, were obtained from the American Type Culture Collection, Manassas, VA, USA). Cells were expanded in Eagle's Minimal Essential Medium (EMEM - ATCC 30-2003) supplemented with penicillin, streptomycin (10,000 U/mL each, Gibco by Life Technologies) and 10% FBS (Gibco by Life Technologies) in 75 mL flasks at 37 °C with 5% atmospheric CO_2. Cells were plated in 24 well plates with a total number of cells of 2.5×10^5 cells for SH-SY5Y and 1.5×10^5 for DU-145 per well and allowed to settle overnight. Differentiation of SH-SY5Y cells was achieved by replacing the medium with a differentiation medium (Dulbecco's modified medium with Ham´s F12 medium (1:1), 1% N2 supplement, 1 μM retinoic acid and 1% PEST). The cells were differentiated for 3 days, and half of the medium in each well was changed every 48 h.

2.3. Epigenetic modulation using 5-Aza-2′-deoxycytidine and trichostatin A

Following the overnight plating, SH-SY5Y and DU-145 cells were treated by replacing the old medium with a fresh layer of medium containing 5-aza-2′-deoxycytidine (Aza dC, 1 μM), Trichostatin A (TSA, 25 nM), a combination of both, or vehicle (DMSO 0.1%) as control. After 24 h, cells were lysed in Dynabeads® mRNA DIRECT™ lysis/binding buffer and frozen at -80 °C. mRNA extraction was performed using the Dynabeads® mRNA DIRECT™ Purification Kit (Thermo Fisher Scientific, Waltham, MA, USA) in accordance with the kit instructions. mRNA extracted from untreated human PC3 prostate cancer cells (obtained from DSMZ (Braunschweig, Germany), cultured in Ham's F-10 medium (Thermo Fisher Scientific), 2 mM L-glutamine, 10% FBS and 1% PEST) were also available at the laboratory.

Table 1
Primers used for qPCR experiments.

Gene	Product	Forward primer (5' to 3')	Reverse primer (5' to 3')
ABHD6	ABHD6	GATGTCCGCATCCCTCATAAC	CCAGCACCTGGTCTTGTTTC
ABHD12	ABHD12	GGCAGAAAGCTCTATAGCATCG	CCTGTAGCCAAGGTCTGAATG
ADARB1 (1)	ADAR2	TTCCCAGTGAGGGTCTTCAG	GACTCCAGCCAGCACTTTTC
ADARB (2)		CCGCCAAGGTACACTGAG	ACAGCTTCGCTAATCCCATC
ALOX5	5-LOX	ATCCAGCTCAACCAAATCCC	ACCAGATGTGTTCGCAGAAG
ALOX12	12-LOX	GATCCGAGGAGAGAAGCAATAC	GGAGGCTGAATCTGGATGAC
ALOX15	15-LOX	CAACTTCCACCAGGCTTCTC	GCCCACAGCCACCATAAC
CNR1	CB_1R	CACCTTCCGCACCATCACCAC	GTCTCCCGCAGTCATCTTCTCTTG
CNR2 (1)	CB_2R	CATGGAGGAATGCTGGGTGAC	GAGGAAGGCGATGAACAGGAG
CNR2 (2)		AAACAACTGGGACTCCTC	GTCTAGAAGGCTTTGGGTTG
DAGLA	DAGLα	CCCAAATGGCGGATCATCG	GGCTGAGAGGGCTATAGTTAGG
DAGLB	DAGLβ	TCAGGTGCTACGCCTTCTC	TCACACTGAGCCTGGGAATC
FAAH	FAAH	CACACGCTGGTTCCCTTCTT	GGGTCCACGAAATCACCTTTGA
MGLL (1)	MAGL	GACAAGACTCTCAAGATTTATGAAGG	TTTATTTCATGGAAGACGGAGTTG
MGLL (2)		GGAAACAGGACCTGAAGACC	ACTGTCCGTCTGCATTGAC
NAAA	NAAA	ATGGAGCGTGGTTCCGAGTT	AGGCTGAGGTTTGCTTGTCCT
NAPEPLD	NAPE-PLD	ACTGGTTATTGCCCTGCTTT	AATCCTTACAGCTTCTTCTGGG
PTGS2	COX-2	AGCAGGCAGATGAAATACCAG	ACCAGAAGGGCAGGATACA
RPL19	RPL19	CACATCCACAAGCTGAAGGCA	CTTGCGTGCTTCCTTGGTCT

Abbreviations for the gene products (unless shown in Fig. 1): ADAR2, adenosine deaminase acting on RNA of the brain glutamate receptor 2 subunit B; RPL19, ribosomal protein L19.

2.4. qPCR measurements

mRNA was extracted using the Dynabeads® mRNA DIRECT™ Purification Kit. mRNA (5 μg) was used for reverse transcription using the High-Capacity cDNA Reverse Transcription Kit with RNase Inhibitor (Applied Biosystems, Thermo Fisher Scientific). The cDNA was diluted 10 times. qPCR reaction mixtures were prepared using the KAPA SYBR FAST qPCR Master Mix (2X, KAPA Biosystems, Wilmington, MA, USA) to a final volume of 20 μL. Reactions were run on the Illumina Eco Real Time PCR system (Illumina Inc, San Diego, CA, USA) with an initial denaturation time of 10 min at 95 °C, 45 cycles of 10 s at 95 °C and 30 s at 60 °C. Primers (Table 1) were designed in-house and synthesized at Integrated DNA Technologies (Coralville, IA, USA). Amounts of transcripts were normalized to ribosomal protein L19 (RPL19). Results are presented as ΔCt as this allows comparison of mRNA levels for the different genes. A difference of +1 or -1 between two groups represents a difference of 50% or 200%, respectively, of the mRNA levels. To aid the reader, the geometric mean values of treated samples are compared as % of the geometric mean control values expressed as $2^{-\Delta\Delta Ct}$, in the Tables.

2.5. [^{3}H]2-OG hydrolysis in SH-SY5Y and DU-145 cells

The assay of Björklund et al. [30] was used, albeit with 2-OG rather than AEA. Cells (2.5×10^5 per well for SH-SY5Y cells and 1.5×10^5 per well for DU-145 cells) were plated and incubated overnight to allow for cell adherence. SH-SY5Y were used the following day while DU-145 cells were incubated for further 24 h to increase confluency before the hydrolysis experiments. In theory, hydrolysis assays could be undertaken by adding substrate to the cells directly. However, FBS contains endocannabinoids that could potentially compete with the substrate for hydrolysis [31], and so the wells were washed with KRH buffer (120 mM NaCl, 4.7 mM KCl, 2.2 mM $CaCl_2.2H_2O$, 10 mM HEPES, 0.12 mM KH_2PO_4, 0.12 mM $MgSO_4$) containing 1% bovine serum albumin followed by KRH buffer alone. KRH buffer containing 0.1% fatty-acid free bovine serum albumin was added to the wells. Inhibitors (URB597 1 μM, JZL184 1 μM, WWL70 10 μM, a combination of URB597, JZL184 and WWL70 and a combination of JZL184 and WWL70 at the aforementioned concentrations) or vehicle (DMSO 0.1-0.15%) were added and plates incubated in a water bath for 10 min at 37 °C. [^{3}H]2-OG (0.5 μM, labelled in the glycerol part of the molecule and diluted with non-radioactive 2-OG to give a final assay concentration of 0.5 μM) was added and plates were incubated for a further 15 min (total reaction volume of 400 μL). The hydrolysis reaction was stopped by adding 600 μL activated charcoal in 0.5 M hydrochloric acid and plates were placed on ice. This allows for the lysis of the cells, and the adsorption of the unmetabolised substrate and the non-radioactive oleic acid by the charcoal. For details of the assay, developed for the hydrolysis of [^{3}H]ethanolamine-labelled AEA, see [32]; and for comparisons of inhibitor potencies with this assay vs. different MAGL assays and/or species, see [33–35]. Charcoal and aqueous phase were separated by centrifugation (2500 rpm, 10 min), 200 μL of the aqueous phase were recovered and mixed with 4 mL scintillation liquid (Ultima Gold, PerkinElmer) for liquid scintillation radioactivity determination with quench correction. Blank values were defined as the tritium recovered from wells not containing cells. For the experiments with the SH-SY5Y cells reported here, the tritium recovered value of (cells-blank)/blank for the vehicle controls was 12 ± 4.2 (mean ± SD, N = 8). The corresponding values for the DU-145 experiments was lower (5.4 ± 1.7, N = 4), but sufficient to ensure assay accuracy. For the control samples, under the conditions used, the tritium recovered – blanks corresponded to 11 ± 2% for the SH-SY5Y cells and 14 ± 1.5% for the DU-145 cells (means ± SD, N = 8 and 4, respectively). Using this assay with rat brain cytosolic preparations, the selective MAGL inhibitor JZL184 [8] produced a maximum ˜90% reduction in the tritium content of the aqueous phase, after subtraction of blank values, with IC_{50} values of 350 and 12 nM following 0 and 30 min of preincubation, respectively [33].

2.6. Statistics

Data are expressed as means ± SD. Two-tailed t-tests not assuming equal variances were determined using the statistical package built into the GraphPad Prism computer programme for the Macintosh (v8.0, GraphPad Software Inc., San Diego, CA, USA). Two-way factorial ANOVA with type II sums of squares and Levene's tests for homogeneity of variances were determined using the function ezANOVA in the package ez version 4.4-0 for the statistical programme R (version 3.5.1). For multiple comparisons, critical values of P were determined using a 5% false discovery rate [36]. For the hydrolysis experiments, a one-way randomized block ANOVA (termed repeated measures ANOVA in the GraphPad Prism programme) has been used since this has been shown in simulation experiments to be more appropriate than a factorial ANOVA when there is a day-to-day variation in the values [37], such as is seen here.

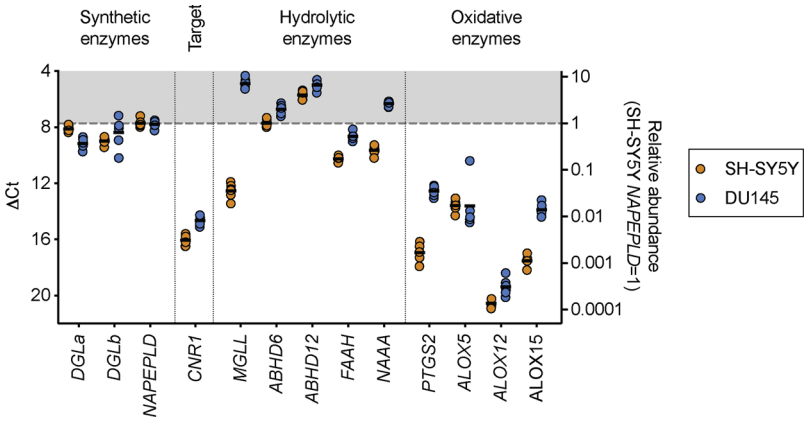

Fig. 2. Relative mRNA abundance for the components of the eCB system in SH-SY5Y and DU145 cells.
Individual ΔCt values are shown, N = 4–6, with the bars indicating the mean ΔCt value, with *RPL19* as standard. (1) and (2) refer to the two different primer pairs used for *MGLL* (see Table 1). The right y-axis shows the mean values expressed relative to the SH-SY5Y *NAPEPLD* levels (chosen because they were the same in the two cell lines) calculated using $2^{-\Delta\Delta Ct}$. The grey area shows higher abundance, the unshaded area lower abundance. The values are taken from the control columns in Tables 2 and 3. For explanation of abbreviations, see Legend to Table 1, and for statistical analysis, see Table 2.

3. Results

3.1. Expression of the components of the endocannabinoid system in SH-SY5Y and DU-145 cells

A total of 15 genes involved in the synthesis, targeting and catabolism of the endocannabinoids (Fig. 1) were investigated at the mRNA level in SH-SY5Y cells. Rather than use a different neuroblastoma line for comparison, we elected to use a non-neural cell line (DU-145 prostate cancer cells). This cell line was chosen because we have previously used it to characterise the effect of an inflammatory cytokine upon the endocannabinoid system and demonstrated expression of the main hydrolytic enzymes for both AEA and 2-AG [38]. We were not able to obtain robust melt curves for either of the two primers for *CNR2,* coding for the CB_2 receptor (data not shown), but good signals were found for the other fourteen genes. The data (which are for the control cells in the epigenetic experiments described in Section 3.3) are shown in Fig. 2, and a statistical evaluation of the data are presented in Table 2. For most of the genes, the relative expression was similar in the two cell lines, but two genes diverged considerably: *PTGS2* (coding for COX-2), which had a ~20-fold higher expression in the DU-145 cells than in the SH-SY5Y cells, and *MGLL*, coding for MAGL, which had a ~200-260 fold higher expression in the DU-145 cells than in the SH-SY5Y cells. Note that we used two different primer pairs for *MGLL*: there are three *MGLL* transcript variants, and our primer pair termed *MGLL(1)* recognised all three transcript variants, whilst the primer pair termed *MGLL(2)* recognised variants 1 and 3, but not 2. The difference in *PTGS2* expression is of marginal interest, given that the expression level *per se* is low in DU-145 cells [38]. However, the low expression of *MGLL* in the SH-SY5Y cells, particularly with respect to the other 2-AG hydrolytic enzymes *ABHD6* [85-fold higher than *MGLL(1)*], *ABHD12* [340-fold higher] and *FAAH* [15-fold higher] was unexpected. In comparison, mRNA levels of *MGLL(1)* were 1.6-fold higher than *ABHD6*, approximately half the levels of *ABHD12* and 6-fold higher than the levels of *FAAH* in DU-145 human prostate cells. With respect to the AEA catabolic enzymes, the levels of *NAAA* and *FAAH* were very similar in the SH-SY5Y cells, albeit slightly lower than in the DU145 cells. Both NAAA and FAAH metabolise *N*-acylethanolamines (of which AEA is a member), although with different hydrolysis rates. Thus, for FAAH, AEA > palmitoylethanolamide (PEA), whereas the reverse is true for NAAA [39,40]. In intact T84 human colon cells, which like the SH-SY5Y cells have an approximately equal expression of *FAAH* and *NAAA*, the hydrolysis of exogenous AEA is brought about entirely by FAAH. The majority of PEA hydrolysis is also sensitive to FAAH inhibition, and inhibition of FAAH, but not of NAAA, increases AEA and PEA levels in interferon-γ-treated T84 cells [41].

One possible explanation for the low expression of *MGLL* in the SH-SY5Y cells is that in their undifferentiated form, the enzyme is not expressed to any great extent, whereas in differentiated neuron-like cells, expression is increased to levels akin to those seen in brain neurons. In order to investigate this, mRNA extracted from undifferentiated and retinoic acid-differentiated SH-SY5Y cells was investigated with respect to *MGLL*, *ABHD6* and *ABHD12* expression, this time with another human prostate cancer cell line, PC3, as a comparison (see [42] for a previous study from our laboratory concerning the uptake and hydrolysis of 2-AG by these cells). The low expression of *MGLL* relative

Table 2
Statistical evaluation of the data shown in Fig. 2.

Gene	Absolute Difference (ΔCt values)			Relative difference	(SH-SY5Y = 1)
	mean	95% CL	P	R^2	
DAGLA	1.03	0.63 to 1.43	0.0003	0.80	0.49
DAGLB	−0.62	−1.73 to 0.48	0.21	0.26	1.54
NAPEPLD	0.06	−0.29 to 0.42	0.69	0.017	0.96
CNR1	−1.41	−1.86 to −0.96	< 0.0001	0.84	2.7
MGLL (1)	−8.05	−9.47 to −6.62	< 0.0001	0.96	264
MGLL (2)	−7.65	−8.26 to −7.05	< 0.0001	0.99	201
ABHD6	−0.99	−1.39 to −0.594	0.0003	0.77	2.0
ABHD12	−0.71	−1.13 to −0.29	0.0037	0.60	1.6
FAAH	−1.60	−1.92 to −1.28	< 0.0001	0.93	3.0
NAAA	−3.34	−3.70 to −2.98	< 0.0001	0.98	10
PTGS2	−4.40	−5.24 to −3.56	< 0.0001	0.97	21
ALOX5	0.02	−2.23 to 2.27	0.98	0.00012	0.99
ALOX12	−1.17	−1.83 to −0.51	0.0036	0.69	2.3
ALOX15	−3.61	−4.38 to −2.85	< 0.0001	0.95	12

The absolute differences are calculated as ΔCt (SH-SY5Y) - ΔCt (DU-145). An absolute difference of -1 corresponds to a relative difference of 2 (i.e. $2^{-(-1)}$). P and R^2 values were obtained from a Welch's t-test. At a 5% false discovery rate, the critical value of P is 0.039.

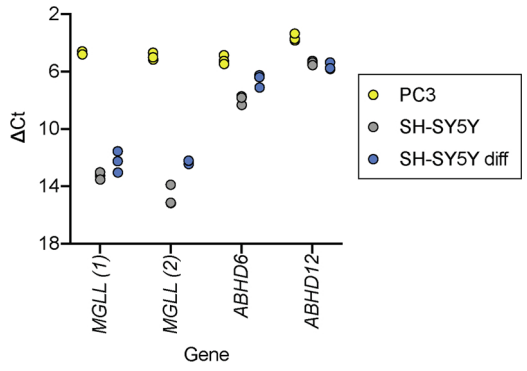

Fig. 3. Relative mRNA abundance for *MGLL*, *ABHD6* and *ADH12* in undifferentiated SH-SY5Y cells, retinoic acid differentiated SH-SY5Y cells and, for comparison in PC3 prostate cancer cells.
Differentiation of the SH-SY5Y cells, confirmed upon morphological inspection of the cells (neurite growth), was achieved using a standard retinoic acid treatment protocol (see Methods). Shown are individual ΔCt values from three experiments. (1) and (2) refer to the two different primer pairs used for *MGLL* (see Table 1).

to *ABHD6* and *ABHD12* in the SH-SY5Y cells (but not in the PC3 cells) was confirmed, and the expression was not increased to any large extent by the differentiation (Fig. 3).

3.2. Hydrolysis of [^{3}H]2-oleoylglycerol by SH-SY5Y and DU-145 cells

In order to determine whether the low expression of *MGLL* relative to *ABHD6* and *ABHD12* in the SH-SY5Y is also reflected at a functional level, intact SH-SY5Y cells were incubated for 15 min with 100 nM [^{3}H]2-OG as MAGL substrate following a 10 min preincubation phase with selective inhibitors of MAGL (1 μM JZL184 [8]), ABHD6 (10 μM WWL70 [43]) and/or FAAH (1 μM URB597 [44]). The rate of 2-OG hydrolysis by human recombinant MAGL is about half of that for 2-AG hydrolysis, but the same is true for human recombinant ABHD12 and ABHD6 [45–47]. The concentration of JZL184 used was 10-fold higher than that used in [29] to obtain a significant protection against MPP^+ toxicity in SH-SY5Y cells. There was a large variation in the inter-experimental observed rate of [^{3}H]2-OG hydrolysis, but potential masking effects of this variation can be dealt with by use of a one-way randomized block ANOVA rather than a factorial ANOVA [37]. Consistent with the mRNA expression, JZL184 per se produced no significant inhibition of [^{3}H]2-OG hydrolysis, whereas a partial inhibition of hydrolysis was seen with WWL70 (Fig. 4A). The combination of JZL184 and WWL70, however, produced a significantly greater inhibition of [^{3}H]2-OG hydrolysis than that seen with WWL70 alone. In the intact DU-145 cells, JZL184 produced a significant inhibition of [^{3}H]2-OG hydrolysis (Fig. 4B).

3.3. Effect of treatment of SH-SY5Y and DU-145 cells with 5-Aza-2′-deoxycytidine (Aza dC) and Trichostatin A (TSA) upon the mRNA expression of endocannabinoid system-related genes

A well-known property of tumour cells is the epigenetic silencing of genes, not least of tumour suppressing genes [48]. In order to determine whether the low *MGLL* expression was a result of epigenetic gene silencing in the SH-SY5Y cells, but not of the DU-145 cells, which are again useful as a comparator since they have a low level of DNA methylcytosine residues [49], the cells were treated with the methylation inhibitor Aza dC and the histone acetylase inhibitor TSA. The concentrations chosen (1 μM and 30 nM, respectively) and the incubation time used (24 h) was the same as in a study of Börner et al. [28], who showed that this treatment increased mRNA expression of *CNR1* in Jurkat cells. No significant changes in mRNA expression levels were seen for any of the genes for either the SH-SY5Y cells (Table 3) or for the DU-145 cells (Table 4). There are literature reports that the mRNA expression in SH-SY5Y of *ALOX15* is increased by TSA and that of *ADARB1* (coding for adenosine deaminase acting on pre-mRNA of the B subunit of the glutamate receptor 2 (ADAR2), unrelated to the endocannabinoid system) by Aza dC, the latter albeit to a modest extent [50,51]. In our hands, *ALOX15* expression is low regardless of treatment, and *ADARB1* expression was not affected by Aza dC and/or TSA (Table 3), the latter regardless as to whether we used the same primer pair as in the study of [50] (termed *ADARB1(1)*, recognises transcript variants 1,2,3,7,9 and 10), or a different primer pair (termed *ADARB1(2)*, recognises transcript variants 3,7,9 and 10 but not 1 or 2).

4. Discussion

SH-SY5Y cells express enzymes associated with catecholaminergic cells [22] and have been used not least to assess potential neuroprotective strategies with respect to Parkinson's disease [23]. With respect to the endocannabinoid system in SH-SY5Y cells, the first study was from Klegeris et al. [26], who found mRNA expression of *CNR1* but not *CNR2* (source of cells from a research colleague). Pasquariello et al. [27] investigated the mRNA expression of *NAPEPLD*, *DAGL*, *CNR1*, *CNR2*, *TRPV1*, *MGLL* and *FAAH* of SH-SY5Y cells and reported a very

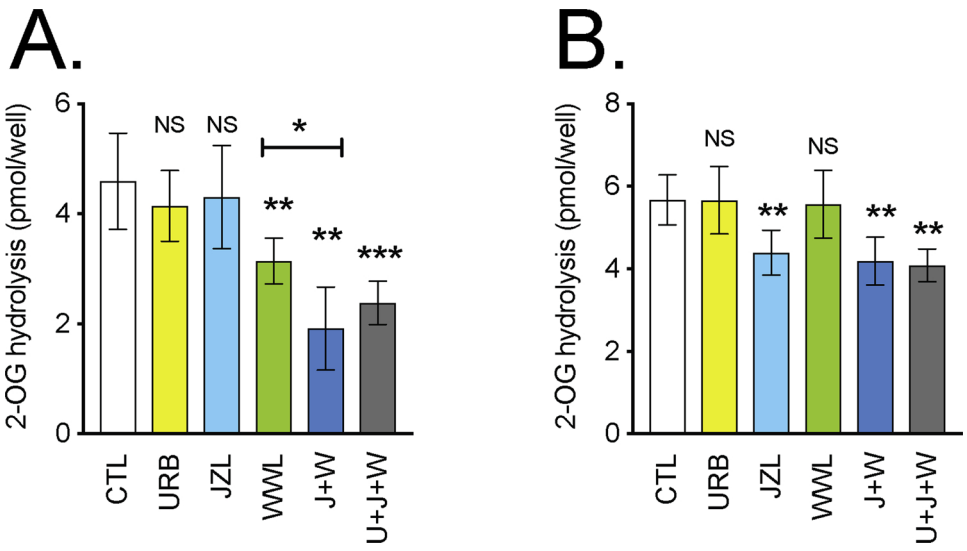

Fig. 4. Hydrolysis of [^{3}H]2-OG by intact SH-SY5Y (Panel A) and DU-145 (Panel B) cells.
Cells were preincubated for 10 min at 37 °C with the inhibitors shown (CTL, vehicle treated control; URB (U), 1 μM URB597; JZL (J), 1 μM JZL184; WWL (W), 10 μM WWL70) or combinations thereof prior to addition of 100 nM [^{3}H]2-OG and incubation for a further 15 min. Data are means ± SD, N = 8 (SH-SY5Y cells) or N = 4 (DU-145 cells). One-way randomized block ANOVAe not assuming sphericity (Geisser-Greenhouse-adjusted degrees of freedom) using the $\log_{10}$-transformed values (since proportional, rather than incremental changes, are expected, see [60]) gave $F_{1.34,9.40} = 22.5$, $P < 0.001$ and $F_{2.05,6.14} = 61.8$, $P < 0.001$ for the SH-SY5Y and DU-145 cells, respectively. ***P < 0.001, **P < 0.01, *P < 0.05, ^{NS}P > 0.05 (after adjustment for a 5% false discovery rate) either vs. the controls or (in Panel A) for the comparison between WWL70 and J + W.

Table 3
Effect of treatment with TSA and Aza dC upon the eCB system in SH-SY5Y cells.

		Vehicle			Aza dC				
		mean[a]	SD	%[b]	mean	SD	%	ANOVA	P value
Synthetic enzymes									
DAGLA	Control	8.13	0.23	100	7.97	0.25	112	Aza dC	0.27
	TSA	8.07	0.21	104	7.97	0.37	111	TSA	0.80
								Aza dC x TSA	0.77
DAGLB	Control	8.99	0.25	100	9.08	0.27	94	Aza dC	0.49
	TSA	9.00	0.36	99	9.08	0.24	94	TSA	0.97
								Aza dC x TSA	0.95
NAPEPLD	Control	7.72	0.28	100	7.63	0.23	106	Aza dC	0.59
	TSA	7.61	0.29	108	7.57	0.26	111	TSA	0.42
								Aza dC x TSA	0.80
Target									
CNR1	Control	16.07	0.38	100	16.34	0.64	83	Aza dC	0.96
	TSA	16.42	0.43	78	16.17	0.54	93	TSA	0.65
								Aza dC x TSA	0.23
Hydrolytic enzymes									
MGLL (1)	Control	14.11	1.33	100	13.53	2.13	150	Aza dC	0.51
	TSA	14.30	0.99	88	14.07	1.22	103	TSA	0.56
								Aza dC x TSA	0.77
MGLL (2)	Control	12.54	0.54	100	12.46	0.51	106	Aza dC	0.83
	TSA	12.62	0.69	95	12.59	0.58	96	TSA	0.66
								Aza dC x TSA	0.90
ABHD6	Control	7.70	0.26	100	7.60	0.25	107	Aza dC	0.18
	TSA	7.77	0.24	95	7.60	0.23	107	TSA	0.71
								Aza dC x TSA	0.71
ABHD12	Control	5.70	0.29	100	5.80	0.34	93	Aza dC	0.74
	TSA	5.71	0.27	99	5.70	0.36	100	TSA	0.75
								Aza dC x TSA	0.69
FAAH	Control	10.24	0.20	100	10.28	0.20	97	Aza dC	0.32
	TSA	10.26	0.17	99	10.37	0.13	92	TSA	0.48
								Aza dC x TSA	0.67
NAAA	Control	9.65	0.33	100	9.48	0.25	113	Aza dC	0.55
	TSA	9.58	0.45	105	9.58	0.32	105	TSA	0.93
								Aza dC x TSA	0.56
Other catabolic enzymes									
PTGS2	Control	16.95	0.69	100	16.62	0.74	126	Aza dC	0.22
(N = 5)	TSA	17.08	0.92	92	16.53	0.69	134	TSA	0.96
								Aza dC x TSA	0.76
ALOX5	Control	13.60	0.41	100	13.58	0.49	102	Aza dC	0.89
	TSA	13.48	0.36	109	13.55	0.19	104	TSA	0.65
								Aza dC x TSA	0.76
ALOX12	Control	20.56	0.31	100	20.33	0.48	117	Aza dC	0.14
	TSA	20.90	0.28	79	20.61	0.39	96	TSA	0.083
								Aza dC x TSA	0.87
ALOX15	Control	17.52	0.50	(N = 4)	18.16	1.32	(N = 5)	Aza dC	0.12
	TSA	17.41	0.35	(N = 4)	18.48	1.48	(N = 6)	TSA	0.79
								Aza dC x TSA	0.69
Other gene									
ADARB1(1)	Control	7.24	0.25	100	7.17	0.38	105	Aza dC	0.87
	TSA	7.16	0.53	106	7.19	0.30	104	TSA	0.86
								Aza dC x TSA	0.74
ADARB1(2)	Control	10.73	0.56	100	11.11	0.85	77	Aza-dC	0.44
	TSA	10.83	0.78	93	11.21	0.42	72	TSA	0.31
								Aza-dC x TSA	0.25

[a] Values are given as ΔCt relative to the housekeeping gene, *RPL19*, and are means ± SD, N = 6, except for *CNR1* and *ALOX12*, where N = 5 and for *ALOX15*, where N = 4-6.

[b] % of the control geometric means, calculated from the geometric mean values as $2^{-\Delta\Delta Ct}$. P values are determined from factorial two-way ANOVAe. In all cases, Levene's test for homogeneity of variance gave P values > 0.05.

low expression of *CNR1* and *CNR2*, a high expression of *TRPV1*, with the other genes being expressed within these two extremes. Although the authors did not specify the source of their SH-SY5Y cells, there is a good agreement on the relative expression levels of the genes studied in [27] and in the present study, with the notable exception of *MGLL*, which was more abundantly expressed in their study (Fig. 5). In another study, Börner et al. [28] reported higher levels of mRNA for *CNR1* (~0.1% of the actin levels) in their SH-SY5Y cells (source of the cells not specified), and low levels of mRNA for *CNR2*. Treatment of the cells with Aza dC and/or TSA, the same concentrations and incubation times as here, did not affect *CNR1* expression but increased *CNR2* expression, the combination of the two agents resulting in *CNR2* expression levels of ~0.1% of the actin levels [28]. Aymerich et al. [29] identified *MGLL*, *CNR1* and *CNR2* in their cells (obtained from ATCC), but did not quantify the signals, other than expressing them as % of vehicle in their experiments. We were unable to quantify *CNR2* levels due to unacceptable melt curves for both of the primers we investigated.

mRNA levels of course do not yield information as to the protein expression or functional activity of enzymes. In this respect, Pasquariello et al. [27] investigated expression using fluorescence microscopy and could demonstrate robust signals for TRPV1, NAPE-PLD and FAAH in the SH-SY5Y cells, whereas no obvious signal was seen for

Table 4
Effect of treatment with TSA and Aza dC upon the eCB system in DU-145 cells.

		Vehicle			Aza dC				
		mean[a]	SD	%[b]	mean[a]	SD	%[b]	ANOVA	P value
Synthetic enzymes									
DAGLA	Control	9.16	0.36	100	9.21	0.35	97	Aza dC	0.44
	TSA	9.13	0.32	102	9.32	0.41	89	TSA	0.77
								Aza dC x TSA	0.65
DAGLB	Control	8.37	1.06	100	8.64	1.20	83	Aza dC	0.59
	TSA	8.63	1.22	83	8.90	1.29	69	TSA	0.60
								Aza dC x TSA	0.99
NAPEPLD	Control	7.79	0.26	100	7.79	0.26	100	Aza dC	0.44
	TSA	7.69	0.34	107	7.89	0.42	93	TSA	0.99
								Aza dC x TSA	0.47
Target									
CNR1	Control	14.66	0.31	100	14.87	0.58	86	Aza dC	0.45
	TSA	14.82	0.58	90	14.93	0.56	83	TSA	0.61
								Aza dC x TSA	0.82
Hydrolytic enzymes									
MGLL (1)	Control	6.07	0.68	100	6.20	0.70	91	Aza dC	0.85
	TSA	5.77	0.91	123	5.52	0.70	146	TSA	0.13
								Aza dC x TSA	0.54
MGLL (2)	Control	4.89	0.37	100	4.95	0.35	96	Aza dC	0.39
	TSA	4.93	0.42	97	5.15	0.39	83	TSA	0.44
								Aza dC x TSA	0.62
ABHD6	Control	6.71	0.35	100	6.77	0.36	96	Aza dC	0.73
	TSA	6.74	0.36	98	6.78	0.41	95	TSA	0.88
								Aza dC x TSA	0.94
ABHD12	Control	4.99	0.35	100	5.16	0.37	89	Aza dC	0.19
	TSA	5.04	0.39	97	5.26	0.30	83	TSA	0.60
								Aza dC x TSA	0.85
FAAH	Control	8.64	0.28	100	8.81	0.23	89	Aza dC	0.063
	TSA	8.69	0.26	97	8.94	0.29	81	TSA	0.42
								Aza dC x TSA	0.71
NAAA	Control	6.31	0.19	100	6.14	0.24	113	Aza dC	0.14
	TSA	6.32	0.25	99	6.19	0.25	108	TSA	0.74
								Aza dC x TSA	0.81
Other catabolic enzyme									
PTGS2	Control	12.55	0.37	100	12.39	0.33	111	Aza dC	0.35
	TSA	12.66	0.25	93	12.55	0.39	100	TSA	0.36
								Aza dC x TSA	0.87
ALOX5	Control	13.62	1.83	100	13.54	1.78	106	Aza dC	0.97
	TSA	13.44	1.79	113	13.58	1.85	103	TSA	0.93
								Aza dC x TSA	0.89
ALOX12	Control	19.39	0.61	100	19.31	0.57	106	Aza dC	0.80
	TSA	19.74	0.68	78	19.70	0.50	81	TSA	0.14
								Aza dC x TSA	0.94
ALOX15	Control	13.90	0.47	100	14.08	0.43	88	Aza dC	0.46
	TSA	13.81	0.60	107	14.01	0.85	93	TSA	0.74
								Aza dC x TSA	0.98
Other gene									
ADARB1(1)	Control	8.16	0.45	100	8.23	0.14	95	Aza dC	0.53
	TSA	8.44	0.60	82	8.13	0.54	102	TSA	0.63
								Aza dC x TSA	0.34
ADARB1 (2)	Control	11.09	0.59	100	11.29	0.42	87	Aza dC	0.71
	TSA	11.24	0.44	90	11.20	0.47	93	TSA	0.89
								Aza dC x TSA	0.55

[a] Values are given as ΔCt relative to the housekeeping gene, *RPL19*, means ± SD, N = 6, except for *ALOX5*, where N = 5.
[b] % of the control geometric means, calculated from the geometric mean values as $2^{-\Delta\Delta Ct}$. P values are determined from factorial two-way ANOVAe. In all cases, Levene's test for homogeneity of variance gave P values > 0.05.

CB_1 receptors. The authors reported a relatively strong immunofluorescence with their CB_2 receptor antibody, but the specificity of the antibody used has been questioned (see [52]). Interestingly, and in contrast to their mRNA data, the MAGL immunoreactivity was not as pronounced as that seen for FAAH. Given our low expression level of *MGLL*, we did not investigate protein expression, since at the expected low levels, signal: noise ratios would be expected to be unacceptable. Instead, we chose to use a functional assay, namely the ability of intact SH-SY5Y cells to catabolise an MAGL substrate, 2-OG. We found no significant effect of the selective MAGL inhibitor JZL184 per se upon 2-OG metabolism in the cells, in contrast to the situation with the DU-145 cells, where the compound significantly inhibited 2-OG hydrolysis. ABHD6 was expressed to a much higher level in the SH-SY5Y cells, and the selective ABHD6 inhibitor produced a partial inhibition of 2-OG hydrolysis. This is reminiscent of the situation in BV2 microglial cells, which do not express MAGL, but utilise ABHD6 to hydrolyse 2-AG [53,54]. Both the BV2 and SH-SY5Y cells are of course cancer-derived. However, in mouse primary neuronal cultures, dual inhibition of FAAH and ABHD6 increases both AEA and 2-AG levels when the neurons are stimulated with glutamate + carbachol [55]. Thus, the contribution of ABHD6 to 2-OG hydrolysis in the SH-SY5Y neuroblastoma cells is not unexpected. Interestingly, the combination of WWL70 and JZL184 produced a greater inhibition in the SH-SY5Y cells than seen with WWL70 alone. This finding is consistent with the possibility that the

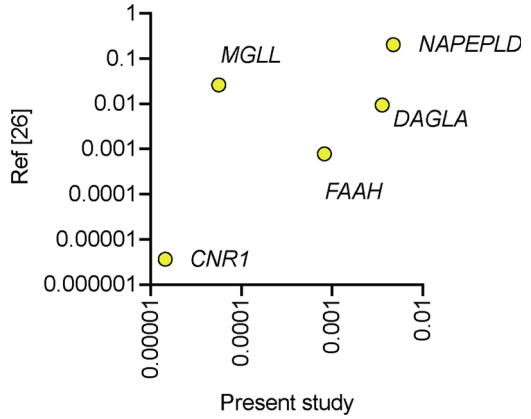

Fig. 5. Comparison of mRNA levels in SH-SY5Y cells between present study and the study of Pasquariello et al. [27].
The data from [27] show the mRNA number of copies relative to actin as housekeeping gene. The authors of that paper referred to *DAGLA* as *DAGL*, but the primer pair used identified *DAGLA* rather than *DAGLB*. The data from the present study is given as $2^{-\text{meanΔCt}}$ relative to *RPL19* as housekeeping gene using *MGLL(1)*.

MAGL activity, although low, can be observed when ABHD6 is inhibited. Further studies are required to explore this tantalising suggestion. It is also notable that there was a considerable residual 2-OG hydrolytic activity even in the presence of the MAGL, ABHD6 and FAAH inhibitors, suggesting that ABHD12 and possibly other hydrolytic enzymes contribute to 2-OG hydrolysis. Certainly, in the mouse brain, ABHD12 is more active than ABHD6 towards 2-AG metabolism [7], but we were not able to investigate this further in the absence of a commercially available ABHD12 inhibitor.

The efficacy of 100 nM JZL184 in reducing the toxic effects of MPP^+ in SH-SY5Y cells [29] is at first sight inconsistent with our data. However, the MPP^+ treatment per se increased expression of both *CNR1* and *CNR2* by ~2.5 and 4-fold, respectively [29], and so it is possible that the treatment also induced *MGLL*, thereby presenting a target for JZL184. The mechanism behind the increases in *CNR* expression were not explored by the authors, but MPP^+-treatment of SH-SY5Y cells increases mRNA expression of the heat shock protein gene *HIF1A* (coding for HIF-1α) [56] and so changes in expression levels of components of the endocannabinoid system may be down-stream of this. MPP^+ treatment of SH-SY5Y cells does not change the global methylation of DNA [57] but does affect methylation of the α-synuclein gene promotor, resulting in an α-synuclein up-regulation [58], and so an effect upon *MGLL* gene expression may in theory be produced in a similar manner. With respect to the endocannabinoid system, treatment of human HCT-117, LS-174 and SW-480 cells with the methylation inhibitor Aza dC increases the expression of CB_1 receptors [59]. In human Jurkat T lymphocyte cells, Aza dC and the histone acetylase inhibitor TSA both increase CB_1 receptor expression [28]. Thus, when taken together, the published data raises the possibility that the low *MGLL* expression in the SH-SY5Y cells seen here under the culturing conditions used was due to epigenetic silencing, in which case the expression should increase dramatically upon treatment with Aza dC and/or TSA. However, this was not the case. In this respect, a large variation in the % of methylated cytosine residues of DNA have been reported in a panel of 70 human cancer cells, with DU-145 cells being one of the lowest. Treatment with 1 μM Aza dC (the concentration used in the present study) for 3–4 days, resulted in an average reduction of cytosine methylation by about half [49]. Cell lines with intrinsically low levels of methylation under the assay conditions used (such as DU-145 cells [49]) would not be expected to show dramatic changes in gene expression after Aza dC treatment, and this may well be the case here, at least with respect to methylation levels in DNA regions related to the genes studied.

In conclusion, the present study has shown that *MGLL* expression in SH-SY5Y cells is very low, and this is reflected in the lack of sensitivity of [^{3}H]-2-OG hydrolysis to inhibition by the selective MAGL inhibitor JZL184. The low *MGLL*, as well as *CNR1*, expression should be taken into account when using these cells in experiments investigating the involvement of the endocannabinoid system in models of physiological and pathological processes. It would certainly be valuable to investigate the expression of *MGLL*, and the activity of MAGL in a range of neuroblastoma cells, both undifferentiated and differentiated, in order to identify potentially useful cell lines for the in vitro study of the protective effects of MAGL inhibitors upon neuroblastoma cell function.

References

[1] V. Di Marzo, New approaches and challenges to targeting the endocannabinoid system, Nat. Rev. Drug Discov. 17 (2018) 623–639.
[2] P. Pacher, S. Bátkai, G. Kunos, The endocannabinoid system as an emerging target of pharmacotherapy, Pharmacol. Rev. 58 (2006) 389–462.
[3] N. Ueda, K. Tsuboi, T. Uyama, Metabolism of endocannabinoids and related *N*-acylethanolamines: Canonical and alternative pathways, FEBS J. 280 (2013) 1874–1894.
[4] D.G. Deutsch, S.A. Chin, Enzymatic synthesis and degradation of anandamide, a cannabinoid receptor agonist, Biochem. Pharmacol. 46 (1993) 791–796.
[5] B.F. Cravatt, K. Demarest, M.P. Patricelli, M.H. Bracey, D.K. Giang, B.R. Martin, A.H. Lichtman, Supersensitivity to anandamide and enhanced endogenous cannabinoid signaling in mice lacking fatty acid amide hydrolase, Proc. Natl. Acad. Sci. U. S. A. 98 (16) (2001) 9371–9376.
[6] S. Goparaju, N. Ueda, H. Yamaguchi, S. Yamamoto, Anandamide amidohydrolase reacting with 2-arachidonoylglycerol, another cannabinoid receptor ligand, FEBS Lett. 422 (1998) 69–73.
[7] J.L. Blankman, G.M. Simon, B.F. Cravatt, A comprehensive profile of brain enzymes that hydrolyze the endocannabinoid 2-arachidonoylglycerol, Chem. Biol. 14 (2007) 1347–1356.
[8] J.Z. Long, W. Li, L. Booker, J.J. Burston, S.G. Kinsey, J.E. Schlosburg, F.J. Pavón, A.M. Serrano, D.E. Selley, L.H. Parsons, A.H. Lichtman, B.F. Cravatt, Selective blockade of 2-arachidonoylglycerol hydrolysis produces cannabinoid behavioral effects, Nat. Chem. Biol. 5 (2009) 37–44.
[9] D.K. Nomura, B.E. Morrison, J.L. Blankman, J.Z. Long, S.G. Kinsey, M.C.G. Marcondes, A.M. Ward, Y.K. Hahn, A.H. Lichtman, B. Conti, B.F. Cravatt, Endocannabinoid hydrolysis generates brain prostaglandins that promote neuroinflammation, Science 334 (2011) 809–813.
[10] A. Viader, J.L. Blankman, P. Zhong, X. Liu, J.E. Schlosburg, C.M. Joslyn, Q.-S. Liu, A.J. Tomarchio, A.H. Lichtman, D.E. Selley, L.J. Sim-Selley, B.F. Cravatt, Metabolic interplay between astrocytes and neurons regulates endocannabinoid action, Cell Rep. 12 (2015) 798–808.
[11] M. Karlsson, J. Contreras, U. Hellman, H. Tornqvist, C. Holm, cDNA cloning, tissue distribution, and identification of the catalytic triad of monoglyceride lipase. Evolutionary relationship to esterases, lysophospholipases, and haloperoxidases, J. Biol. Chem. 272 (43) (1997) 27218–27223.
[12] N.T. Snider, V.J. Walker, P.F. Hollenberg, Oxidation of the endogenous cannabinoid arachidonoyl ethanolamide by the cytochrome p450 monooxygenases: physiological and pharmacological implications, Pharmacol. Rev. 62 (1) (2010) 136–154.
[13] D.K. Nomura, J.Z. Long, S. Niessen, H.S. Hoover, S.-W. Ng, B.F. Cravatt, Monoacylglycerol lipase regulates a fatty acid network that promotes cancer pathogenesis, Cell 140 (1) (2010) 49–61.
[14] M. Alhouayek, D.M. Lambert, N.M. Delzenne, P.D. Cani, G.G. Muccioli, Increasing endogenous 2-arachidonoylglycerol levels counteracts colitis and related systemic inflammation, FASEB J. 25 (8) (2011) 2711–2721.
[15] G. Hernández-Torres, M. Cipriano, E. Hedén, E. Björklund, A. Canales, D. Zian, A. Feliú, M. Mecha, C. Guaza, C.J. Fowler, S. Ortega-Gutiérrez, M.L. López-Rodríguez, A reversible and selective inhibitor of monoacylglycerol lipase ameliorates multiple sclerosis, Angew. Chem. 53 (2014) 13765–13770.
[16] G. Bedse, R.J. Bluett, T.A. Patrick, N.K. Romness, A.D. Gaulden, P.J. Kingsley, N. Plath, L.J. Marnett, S. Patel, Therapeutic endocannabinoid augmentation for mood and anxiety disorders: comparative profiling of FAAH, MAGL and dual inhibitors, Transl. Psychiatry 8 (2018) 92.
[17] S.O. Alapafuja, M.S. Malamas, V. Shukla, A. Zvonok, S. Miller, L. Daily, G. Rajarshi, C.Y. Miyabe, H. Chandrashekhar, J.A. Wood, S. Tyukhtenko, A. Straiker, A. Makriyannis, Synthesis and evaluation of potent and selective MGL inhibitors as a glaucoma treatment, Bioorg. Med. Chem. 27 (2019) 55–64.
[18] R.B. Mounsey, S. Mustafa, L. Robinson, R.A. Ross, G. Riedel, R.G. Pertwee, P. Teismann, Increasing levels of the endocannabinoid 2-AG is neuroprotective in the 1-methyl-4-phenyl-1,2,3,6-tetrahydropyridine mouse model of Parkinson's disease, Exp. Neurol. 273 (2015) 36–44.
[19] N. Pasquarelli, C. Porazik, H. Bayer, E. Buck, S. Schildknecht, P. Weydt, A. Witting, B. Ferger, Contrasting effects of selective MAGL and FAAH inhibition on dopamine depletion and GDNF expression in a chronic MPTP mouse model of Parkinson's disease, Neurochem. Int. 110 (2017) 14–24.
[20] P. Shastry, A. Basu, M.S. Rajadhyaksha, Neuroblastoma cell lines - a versatile in vitro model in neurobiology, Int. J. Neurosci. 108 (2001) 109–126.

[21] J.L. Biedler, S. Roffler-Tarlov, M. Schrachner, L.S. Freedman, Multiple neurotransmitter synthesis by human neuroblastoma cell lines and clones, Cancer Res. 38 (1978) 3751–3757.
[22] J.A. Korecka, R.E. van Kesteren, E. Blaas, S.O. Spitzer, J.H. Kamstra, A.B. Smit, D.F. Swaab, J. Verhaagen, K. Bossers, Phenotypic characterization of retinoic acid differentiated SH-SY5Y cells by transcriptional profiling, PLoS One 8 (2013) e63862.
[23] H. Xicoy, B. Wieringa, G.J.M. Martens, The SH-SY5Y cell line in Parkinson's disease research: a systematic review, Mol Neurodegenerat 12 (2017) 10.
[24] M. Maccarrone, T. Lorenzon, M. Bari, G. Melino, A. Finazzi-Agrò, Anandamide induces apoptosis in human cells via vanilloid receptors. Evidence for a protective role of cannabinoid receptors, J. Biol. Chem. 275 (41) (2000) 31938–31945.
[25] M. Maccarrone, M. Attinà, A. Cartoni, M. Bari, A. Finazzi-Agrò, Gas chromatography - mass spectrometry analysis of endogenous cannabinoids in healthy and tumoral human brain and human cells in culture, J. Neurochem. 76 (2) (2001) 594–601.
[26] A. Klegeris, C.J. Bissonnette, P.L. McGeer, Reduction of human monocytic cell neurotoxicity and cytokine secretion by ligands of the cannabinoid-type CB_2 receptor, Br. J. Pharmacol. 139 (2003) 775–786.
[27] N. Pasquariello, G. Catanzaro, V. Marzano, D. Amadio, D. Barcaroli, S. Oddi, G. Federici, A. Urbani, A. Finazzi Agrò, M. Maccarrone, Characterization of the endocannabinoid system in human neuronal cells and proteomic analysis of anandamide-induced apoptosis, J. Biol. Chem. 284 (43) (2009) 29413–29426.
[28] C. Börner, E. Martella, V. Höllt, J. Kraus, Regulation of opioid and cannabinoid receptor genes in human neuroblastoma and T cells by the epigenetic modifiers trichostatin A and 5-aza-2'-deoxycytidine, Neuroimmunomodulation 19 (3) (2012) 180–186.
[29] M.S. Aymerich, E. Rojo-Bustamante, C. Molina, M. Celorrio, J.A. Sánchez-Arias, R. Franco, Neuroprotective effect of JZL184 in MPP^+-treated SH-SY5Y cells through CB_2 receptors, Mol. Neurobiol. 53 (2016) 2312–2319.
[30] E. Björklund, A. Blomqvist, J. Hedlin, E. Persson, C.J. Fowler, Involvement of fatty acid amide hydrolase and fatty acid binding protein 5 in the uptake of anandamide by cell lines with different levels of fatty acid amide hydrolase expression: a pharmacological study, PLoS One 9 (2014) e103479.
[31] J. Marazzi, J. Kleyer, J.M.V. Paredes, J. Gertsch, Endocannabinoid content in fetal bovine sera - Unexpected effects on mononuclear cells and osteoclastogenesis, J. Immunol. Methods 373 (1–2) (2011) 219–228.
[32] L. Boldrup, S.J. Wilson, A.J. Barbier, C.J. Fowler, A simple stopped assay for fatty acid amide hydrolase avoiding the use of a chloroform extraction phase, J. Biochem. Biophys. Methods 60 (2) (2004) 171–177.
[33] E. Björklund, E. Norén, J. Nilsson, C.J. Fowler, Inhibition of monoacylglycerol lipase by troglitazone, *N*-arachidonoyl dopamine and the irreversible inhibitor JZL184: comparison of two different assays, Br. J. Pharmacol. 161 (2010) 1512–1526.
[34] J.A. Cisneros, E. Björklund, I. González-Gil, Y. Hu, A. Canales, F.J. Medrano, A. Romero, S. Ortega-Gutiérrez, C.J. Fowler, M.L. López-Rodríguez, Structure-activity relationship of a new series of reversible dual monoacylglycerol lipase/fatty acid amide hydrolase inhibitors, J. Med. Chem. 55 (2) (2012) 824–836.
[35] R. Cheng, M. Mori, L. Ma, M. Alhouayek, A. Hatori, Y. Zhang, D. Ogasawara, G. Yuan, Z. Chen, X. Zhang, H. Shi, T. Yamasakin, L. Xie, K. Kumata, M. Fujinaga, Y. Nagai, T. Minamimoto, M. Svensson, L. Wang, Y. Du, M.J. Ondrechen, N. Vasdev, B. Cravatt, C. Fowler, M.-R. Zhang, S.H. Liang, Site-specific ^{11}C-labeled azetidine carboxylates reveal mechanistic insights for binding to monoacylglycerol lipase by PET imaging studies, J. Med. Chem. 61 (2018) 2278–2291.
[36] Y. Benjamini, Y. Hochberg, Controlling the false discovery rate: a practical and powerful approach to multiple testing, J. R. Stat. Soc. B 57 (1995) 289–300.
[37] M. Lew, Good statistical practice in pharmacology. Problem 2, Br. J. Pharmacol. 152 (2007) 299–303.
[38] J. Karlsson, S. Gouveia-Figueira, M. Alhouayek, C.J. Fowler, Effects of tumour necrosis factor α upon the metabolism of the endocannabinoid anandamide in prostate cancer cells, PLoS One 12 (2017) e0185011.
[39] S. Maurelli, T. Bisogno, L. De Petrocellis, A. Luccia, G. Marino, V. Di Marzo, Two novel classes of neuroactive fatty acid amides are substrates for mouse neuroblastoma' anandamide amidohydrolase', FEBS Lett. 377 (1995) 82–86.
[40] N. Ueda, K. Yamanaka, S. Yamamoto, Purification and characterization of an acid amidase selective for *N*-palmitoylethanolamine, a putative endogenous anti-inflammatory substance, J. Biol. Chem. 276 (2001) 35552–35557.
[41] M. Alhouayek, L. Rankin, S. Gouveia-Figueira, C.J. Fowler, Interferon γ treatment increases endocannabinoid and related *N*-acylethanolamine levels in T84 human colon carcinoma cells, Br. J. Pharmacol. (2019) in press (http://rdcu.be/GVQt).
[42] C.J. Fowler, N. Ghafouri, Does the hydrolysis of 2-arachidonoylglycerol regulate its cellular uptake? Pharmacol. Res. 58 (1) (2008) 72–76.
[43] W. Li, J.L. Blankman, B.F. Cravatt, A functional proteomic strategy to discover inhibitors for uncharacterized hydrolases, J. Am. Chem. Soc. 129 (2007) 9594–9595.
[44] S. Kathuria, S. Gaetani, D. Fegley, F. Valiño, A. Duranti, A. Tontini, M. Mor, G. Tarzia, G. La Rana, A. Calignano, A. Giustino, M. Tattoli, M. Palmery, V. Cuomo, D. Piomelli, Modulation of anxiety through blockade of anandamide hydrolysis, Nat. Med. 9 (2003) 76–81.
[45] D. Navia-Paldanius, J.R. Savinainen, J.T. Laitinen, Biochemical and pharmacological characterization of human α/β-hydrolase domain containing 6 (ABHD6) and 12 (ABHD12), J. Lipid Res. 53 (2012) 2413–2424.
[46] T. Laitinen, D. Navia-Paldanius, R. Rytilahti, J.J. Marjamaa, J. Karřízková, T. Parkkari, T. Pantsar, A. Poso, J.T. Laitinen, J.R. Savinainen, Mutation of cys242 of human monoacylglycerol lipase disrupts balanced hydrolysis of 1- and 2-monoacylglycerols and selectively impairs inhibitor potency, Mol. Pharmacol. 85 (2014) 510–519.
[47] A. Joshi, M. Shaikh, S. Singh, A. Rajendran, A. Mhetre, S.S. Kamat, Biochemical characterization of the PHARC-associated serine hydrolase ABHD12 reveals its preference for very-long-chain lipids, J. Biol. Chem. 293 (2018) 16953–16963.
[48] P.A. Jones, S.B. Baylin, The epigenomics of cancer, Cell 128 (2007) 683–692.
[49] M.F. Paz, M.F. Fraga, S. Avila, M. Gui, M. Pollan, J.G. Herman, M. Esteller, A systematic profile of DNA methylation in human cancer cell lines, Cancer Res. 63 (2003) 1114–1121.
[50] H. Uchida, S. Ito, Differential regulation of expression of RNA-editing enzymes, ADAR1 and ADAR2, by 5-aza-2′-deoxycytidine and trichostatin A in human neuronal SH-SY5Y cells, NeuroReport 26 (2015) 1089–1094.
[51] C.F.-Y. Ho, C.P.-E. Bon, Y.-K. Ng, D.R. Herr, J.-S. Wu, T.-N. Lin, W.-Y. Ong, Expression of DHA-metabolizing enzyme Alox15 is regulated by selective histone acetylation in neuroblastoma cells, Neurochem. Res. 43 (2018) 540–555.
[52] Y. Marchalant, P.W. Brownjohn, A. Bonnet, T. Kleffmann, J.C. Ashton, Validating antibodies to the cannabinoid CB_2 Receptor: antibody sensitivity is not evidence of antibody specificity, J. Histochem. Cytochem. 62 (2014) 395–404.
[53] W.R. Marrs, J.L. Blankman, E.A. Horne, A. Thomazeau, Y.H. Lin, J. Coy, A.L. Bodor, G.G. Muccioli, S.S.-J. Hu, G. Woodruff, S. Fung, M. Lafourcade, J.P. Alexander, J.Z. Long, W. Li, C. Xu, T. Möller, K. Mackie, O.J. Manzoni, B.F. Cravatt, N. Stella, The serine hydrolase ABHD6 controls the accumulation and efficacy of 2-AG at cannabinoid receptors, Nat. Neurosci. 13 (8) (2010) 951–957.
[54] G. Muccioli, C. Xu, E. Odah, E. Cudaback, J. Cisneros, D. Lambert, M. López-Rodríguez, S. Bajjalieh, N. Stella, Identification of a novel endocannabinoid-hydrolyzing enzyme expressed by microglial cells, J. Neurosci. 27 (2007) 2883–2889.
[55] W.R. Marrs, E.A. Horne, S. Ortega-Gutierrez, J.A. Cisneros, C. Xu, Y.H. Lin, G.G. Muccioli, M.L. Lopez-Rodriguez, N. Stella, Dual inhibition of α/ß-hydrolase domain 6 and fatty acid amide hydrolase increases endocannabinoid levels in neurons, J. Biol. Chem. 286 (2011) 28723–28728.
[56] S.-Y. Dong, Y.-J. Guo, Y. Feng, X.-X. Cui, S.-H. Kuo, T. Liu, Y.-C. Wu, The epigenetic regulation of HIF-1α by SIRT1 in MPP^+ treated SH-SY5Y cells, Biochem. Biophys. Res. Commun. 470 (2016) 453–459.
[57] B. Benassi, S. Santangeli, C. Merla, L. Tarantini, V. Bollati, A. Butera, C. Marino, C. Consales, 50-HZ MF does not affect global DNA methylation of SH-SY5Y cells treated with the neurotoxin MPP^+, Bioelectromagnetics 40 (2019) 33–41.
[58] J. Yang, Z. Yang, X. Wang, M. Suna, Y. Wang, X. Wang, CpG demethylation in the neurotoxicity of 1-methyl-4-phenylpyridinium might mediate transcriptional upregulation of α-synuclein in SH-SY5Y cells, Neurosci. Lett. 659 (2017) 124–132.
[59] D. Wang, H. Wang, W. Ning, M. Backlund, S. Dey, R. DuBois, Loss of cannabinoid receptor 1 accelerates intestinal tumor growth, Cancer Res. 68 (2008) 6468–6476.
[60] GraphPad Statistics Guide. Paired or ratio t-test. https://www.graphpad.com/guides/prism/7/statistics/index.htm?stat_paired_or_ratio_t_test.htm (URL verified 29 March 2019).